Dicle University
Journal of Engineering
https://dergipark.org.tr/tr/pub/dumf
duje.dicle.edu.tr

Research Article

Dynamic Model and Control of an Electric Vehicle with Four In-Wheel PMSMs

Merve YILDIRIM[1*], Eyyup OKSUZTEPE[2], Hasan KURUM[3]

[1] Firat University, Department of Electrical and Electronics Engineering, merveyildirim@firat.edu.tr, Orcid No: 0000-0003-1284-7324
[2] Firat University, School of Aviation, eoksuztepe@firat.edu.tr, Orcid No: 0000-0002-5446-4308
[3] Biruni University, Department of Electrical and Electronics Engineering, hkurum@biruni.edu.tr, Orcid No: 0000-0002-5498-6819

ARTICLE INFO

Article history:

Received 28 May 2024
Received in revised form 30 June 2024
Accepted 29 July 2024
Available online 30 September 2024

Keywords:

Electric vehicle, permanent magnet synchronous motor, dynamic model, motor control.

Doi: 10.24012/dumf.1491154

* Corresponding author

ABSTRACT

In this paper, a dynamic modeling and control of an Electric Vehicle (EV) with four In-Wheel Permanent Magnet Synchronous Motors (IW-PMSM) are realized by using MATLAB/Simulink. In automotive applications especially in the EVs, PMSMs are generally utilized due to significant features such as high efficiency, high power density, and fast torque response. For this reason, they are also preferred in this study. Four PMSMs are fitted into the wheels to distribute power evenly for each wheel and thus, each motor can be controlled independently. In the dynamic model of the EV, all lateral and longitudinal forces acting on the EV are calculated. Besides, four wheel speeds are estimated according to the designed an Electronic Differential System (EDS) based the speed of the vehicle and steering angle. Then, a PID controller is designed so that the difference in the wheel speed values taken from the EDS is equal to the difference in the speeds taken from the actual system. The speed curve of each wheel and the road curve of the EV are drawn for different steering angles. As a result, it is observed that the stability of the EV is provided for various road conditions. Besides, complexity of the system is reduced by the proposed simpler control technique than the other methods in the literature such as fuzzy logic, direct torque control, and sliding mode control.

Introduction

Nowadays, increasing the number of the vehicles causes the air and environmental pollution. To prevent this, the use of Electric Vehicles (EVs) has become widespread. In addition to environmental awareness, the EVs have other significant advantages such as reliability, comfortable driving, low maintenance cost, and low fuel cost, etc. [1, 2].

EVs are complex systems requiring kinematic and dynamic modelling. Therefore, using right control techniques are quite important for controlling the EV [3]. When the EV is going on a road, all vehicle dynamics including lateral and longitudinal forces should be considered to provide the stability of the EV. Besides, the speed of each wheel of a four-wheel drive EV should also be controlled separately. Accordingly, using various control methods, the speed controller is realized and the speed regulation is ensured.

Many studies have been examined on the dynamic model and control strategies of the EV in the literature. First of all proposes a path tracking control of a four-wheel drive EV using a Model Predictive Control (MPC) method [4]. The nonlinear dynamical model of the EV is converted as a linear model for a MPC design. Then, the EV is provided to follow the reference path based on the reference yaw angle and longitudinal displacement. It is aimed by this study that the error between the reference and measurement results is decreased by the MPC method. Thus, a good path tracking performance for an EV with four wheel is obtained and the road stability is provided. In [5], a lateral control and yaw stability control are handled by differential braking. The vehicle yaw moment may be generated by the differential braking. This changes the lateral position and yaw rate of the vehicle. For this reason, a fuzzy logic controller is proposed for lateral control and yaw stability control. Thus, the response time is reduced for the lateral and yaw errors and a stabile vehicle system is designed. [6, 7] presents a vehicle motion control strategy for the EVs with four in-wheel motors. A control allocation examining the effect of the longitudinal force on the lateral force is proposed. As a result, the longitudinal forces of the wheels are set optimally using Quadratic Programming technique and an efficient system is designed. In [8], a modelling and simulation of an EV are realized using a Simcenter Amesim platform. The dynamic and quasi-static battery models of the EV are examined. Using the speed of the EV, the simulation results are validated with the experimental results. Authors in [9] study estimation of sideslip and roll angles of the EVs using lateral tire force sensors. To measure the sideslip a Recursive Least Squares (RLS) algorithm is utilized. Kalman filter is also preferred for

the roll angle calculation. The simulation results are tested on an experimental EV. It is observed that the roll angle and sideslip angle are estimated with high accuracy. The direct yaw moment control is presented for the in-wheel EVs in [10]. The sideslip angle is estimated by using a state observer. For this purpose, a discontinuous sliding mode direct yaw-moment controller is designed to set the sideslip angle and the yaw rate optimally. In [11], a trajectory tracking control is proposed for four-wheel drive EV utilizing Model Predictive Control (MPC) and Sliding Model Control (SMC) methods. Active front steering and direct yaw moment are examined for high speed situations of the EV. While the MPC technique provides the optimal tracking trajectory, the SMC reduces the large chattering issue in the traditional First-Order Sliding Mode Control (FOSMC). Therefore, the road stability is ensured for high speeds of the EV by this study. Another study presents an Acceleration Slip Regulation (ASR) control for an EV driven by two-wheel independently based on dynamic torque distribution [12]. The single wheel ASR based on fuzzy control is realized using Matlab/Simulink. It is shown from the simulation results that the lateral stability and dynamic tracking capability are better than traditional ASR. An electronic stability control based on motor driving and braking torque distribution for an EV driven by four in-wheel motors in [13]. The yaw rate and sideslip angle of the EV are controlled for the vehicle stability. The torque distribution algorithm is used to generate driving torque or regenerative braking torque of each motor. The proposed method is simulated by using Matlab/Simulink and it is implemented to a CarSim vehicle model. It is obtained from the simulation results that the lateral stability of the EV is provided by utilizing the torque distribution strategies.

When examining the studies in the literature, it is observed that there are a lot of control methods for the vehicle stability. These methods are complex techniques and they increase transaction complexity. For this reason, in this study, a simpler PID controller approach is proposed. A dynamic model including the tire and vehicle dynamics, an EDS, four IW-PMSMs and drives is designed. Here, the PMSMs are fitted into the wheels to provide independent control of each wheel. Thus, the torque is distributed equally to each wheel. The speeds of the front and rear wheels are calculated for various steering angles and speeds of the EV in the EDS. Then, the actual system speeds of the EV are synchronized to the reference speeds taken from the EDS. In conclusion, a stable system is designed for an EV with four IW-PMSMs and safe driving is provided for different road conditions.

The paper consists of six parts. Firstly, the PMSMs under subheadings which are their topology, dynamic model, and control are explained in Section 2. Then, a dynamic model of the EV is examined in Section 3. The control of the EV with four IW-PMSMs is realized in Section 4. After that, the results and discussions are handled in Section 5. The conclusions are given in Section 6.

Permanent Magnet Synchronous Motors

Topology

Synchronous motors are constant speed machines that always rotate at synchronous speed depending on the frequency of the source and the number of poles of the motor. Alternative current is applied to its stators and direct current is applied to its rotors. Thus, it is double excited since two separate magnetic fields are produced [14].

In the brushed DC motors, a smooth torque is obtained by constantly changing the direction of the rotor current with the brush collector structure. In the brushless DC motors and PMSMs, a magnetic field is created thanks to the permanent magnets in the rotor [15]. This provides significant advantages. Since there are no excitation windings, it reduces losses. Therefore, their efficiency is high. Since their size is small, their moment/volume ratio is higher [16]. Additionally, since there is no brush and collector, their structure is simpler and maintenance costs are low.

Dynamic model of the PMSMs

The mathematical model of an PMSM is similar to a wound rotor synchronous motor. It is obtained by considering some assumptions which are negligence of the saturation, eddy currents and hysteresis losses, the skin effect of the current, not being the cage in the rotor and field current dynamics, inductance and resistance values not affected by temperature, and having a sinusoidal induced EMF. The permanent magnets used in the PMSM are a modern rare earth variety with high resistance. Therefore, the currents induced in the rotor can be neglected [17, 18].

The three-phase model of a Y-connected three-phase PMSM is derived using the equivalent circuit given in Fig. 1.

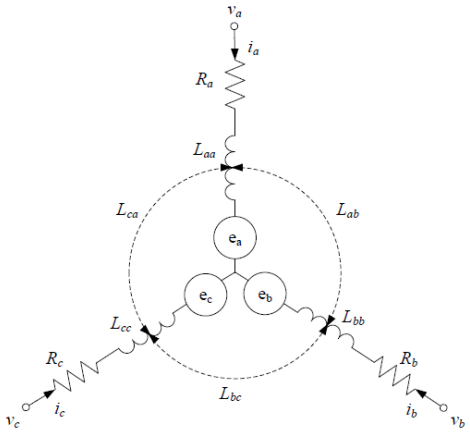

Figure 1. Three-phase equivalent circuit of the PMSM [19].

Using the equivalent circuit in Fig. 1, the three-phase voltages of the PMSM are shown in Equation (1).

$$\begin{bmatrix} V_a \\ V_b \\ V_c \end{bmatrix} = \begin{bmatrix} R_a & 0 & 0 \\ 0 & R_b & 0 \\ 0 & 0 & R_c \end{bmatrix} \begin{bmatrix} i_a \\ i_b \\ i_c \end{bmatrix} + \begin{bmatrix} L_{aa} & L_{ab} & L_{ca} \\ L_{ab} & L_{bb} & L_{bc} \\ L_{ca} & L_{bc} & L_{cc} \end{bmatrix} \frac{d}{dt} \begin{bmatrix} i_a \\ i_b \\ i_c \end{bmatrix} + \begin{bmatrix} e_a \\ e_b \\ e_c \end{bmatrix} \quad (1)$$

where V_a, V_b, V_c are stator voltages for the phases a, b, c, i_a, i_b, and i_c are the stator currents, R_a, R_b, and R_c are the phase winding resistances, e_a, e_b, and e_c are back EMFs induced in the stator, L_{aa}, L_{bb}, and L_{cc} are total inductances of the phase windings, L_{ab}, L_{bc}, and L_{ca} are the mutual inductances between

the phases. R_a, R_b and R_c are the phase resistances which are equal to each other and it can be expressed as R_s.

If the voltage equation given in Equation (2) is rearranged with the magnetic fluxes ψ_a, ψ_b, and ψ_c as follows

$$\begin{bmatrix} V_a \\ V_b \\ V_c \end{bmatrix} = \begin{bmatrix} R_a & 0 & 0 \\ 0 & R_b & 0 \\ 0 & 0 & R_c \end{bmatrix} \begin{bmatrix} i_a \\ i_b \\ i_c \end{bmatrix} + \frac{d}{dt} \begin{bmatrix} \psi_a \\ \psi_b \\ \psi_c \end{bmatrix} \quad (2)$$

L_{ss} which is the phase winding total inductance and mutual inductance M can be calculated as follows

$$L_{ss} = L_{aa} = L_{bb} = L_{cc} = L_1 + L_{ms} \quad (3)$$

$$M = L_{ab} = L_{bc} = L_{ca} = -\frac{1}{2} L_{ms} \quad (4)$$

where L_1, L_{ms}, and M are the leakage inductance, the phase winding self-inductance, and mutual inductance between the phases.

Using these inductances, the fluxes for the phases a, b, c can be found in Equation (5).

$$\begin{bmatrix} \psi_a \\ \psi_b \\ \psi_c \end{bmatrix} = \begin{bmatrix} L_{ss} & M & M \\ M & L_{ss} & M \\ M & M & L_{ss} \end{bmatrix} \begin{bmatrix} i_a \\ i_b \\ i_c \end{bmatrix} + \begin{bmatrix} \lambda_f \cos\theta_r \\ \lambda_f \cos(\theta_r - \frac{2\pi}{3}) \\ \lambda_f \cos(\theta_r - \frac{4\pi}{3}) \end{bmatrix} \quad (5)$$

where λ_f is the back EMF constant and θ_r is the rotor position.

When the voltage equation is rearranged according to the magnetic fluxes, it can be expressed as follows

$$\begin{bmatrix} V_a \\ V_b \\ V_c \end{bmatrix} = \begin{bmatrix} R_s & 0 & 0 \\ 0 & R_s & 0 \\ 0 & 0 & R_s \end{bmatrix} \begin{bmatrix} i_a \\ i_b \\ i_c \end{bmatrix} + \begin{bmatrix} L_{ss} & M & M \\ M & L_{ss} & M \\ M & M & L_{ss} \end{bmatrix} \frac{d}{dt} \begin{bmatrix} i_a \\ i_b \\ i_c \end{bmatrix} - \omega_r \begin{bmatrix} \lambda_f \sin\theta_r \\ \lambda_f \sin(\theta_r - \frac{2\pi}{3}) \\ \lambda_f \sin(\theta_r - \frac{4\pi}{3}) \end{bmatrix} \quad (6)$$

Three phase voltages and stator flux linkages are converted into the d, q axis values as given below, respectively [20].

$$V_d = R i_d + p\lambda_d + \omega_s \lambda_d \quad (7)$$

$$V_q = R i_q + p\lambda_q + \omega_s \lambda_q \quad (8)$$

$$\lambda_d = L_d i_d + \lambda_{af} \quad (9)$$

$$\lambda_q = L_q i_q \quad (10)$$

where V_d and V_q are d-q axis voltages, i_d and i_q are d-q axis stator currents, L_d and L_q are d-q axis inductances, λ_d and λ_q are d-q axis stator flux relations. R, ω_s, and λ_{af} are the stator resistance, synchronous speed, and the flux due to the rotor magnets ringing the stator.

Torque equation for the motor dynamics can be given in Equation (11).

$$T_e = T_L + B\omega_r + j\, p\, \omega_r \quad (11)$$

P, T_L, B, ω_r, and j the number of the pole pairs, load torque, damping coefficient, rotor speed, and moment of inertia, respectively.

Due to the nonlinear machine model, the dynamic equations of the PMSM can be derived as follows

$$p\, i_d = (V_d - R i_d + \omega_s L_q i_q) / L_d \quad (12)$$

$$p\, i_q = (V_q - R i_q - \omega_s L_d i_d - \omega_s \lambda_{af}) / L_q \quad (13)$$

$$p\, \omega_r = (T_e - T_L - B\omega_r) / j \quad (14)$$

The d-q voltages can be obtained from the Park transform in Equation (15).

$$\begin{bmatrix} V_q \\ V_d \\ V_0 \end{bmatrix} = 2/3 \begin{bmatrix} \cos\theta & \cos(\theta - \frac{2\pi}{3}) & \cos(\theta + \frac{2\pi}{3}) \\ \sin\theta & \sin(\theta - \frac{2\pi}{3}) & \sin(\theta + \frac{2\pi}{3}) \\ \frac{1}{2} & \frac{1}{2} & \frac{1}{2} \end{bmatrix} \begin{bmatrix} V_a \\ V_b \\ V_c \end{bmatrix} \quad (15)$$

The total input power of the PMSM is calculated as follows

$$P_T = 3(v_d i_d + v_q i_q) / 2 \quad (16)$$

Control of the PMSM

In this study, an Interior PMSM (IPMSM) is used. The block diagram of the motor speed control of IPMSM is shown in Fig. 2. Here, the reference speed (*) indicates the angular speed value at which the motor is desired to rotate. Therefore, torque adjustment can be made.

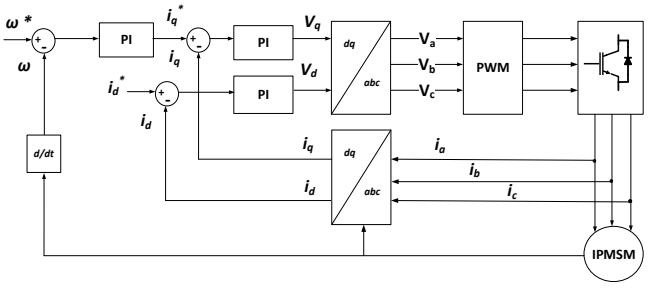

Figure 2. The speed control diagram of the IPMSM.

In the system, the reference speed value is compared with the actual speed, the error value is passed through the PI controller and the reference value i_q* of the i_q current is found. i_q* is compared with the actual current value i_q and the error current is passed through the PI controller to obtain the V_q voltage signal. Likewise, by comparing the reference current i_d* with the actual current value i_d, the error current is passed through the PI controller and the V_d voltage signal is obtained. The

found V_d and V_q voltages are converted into *a, b, c* voltages by Inverse Park and Clarke transformations to obtain the three-phase voltage signals required for the motor. Thus, PWM signals are generated and given as a reference to the voltage source inverter, ensuring that the motor follows the reference speed.

Dynamic model of the EV

The dynamic model of an EV with a four-wheel drive is shown in Fig. 3. Here, *F* is the force of the each wheel and *D* is the lateral slip force based on turning movement of the EV.

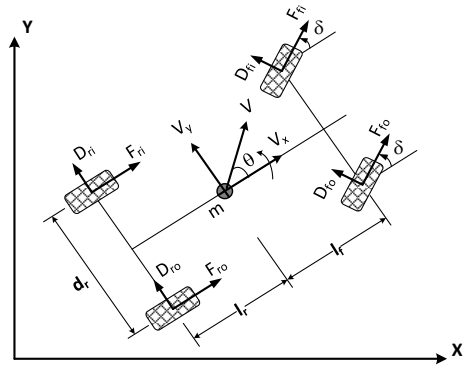

Figure 3. A dynamic model of the EV with a four-wheel drive [21]

A mathematical model of the EV is derived from the Newton second motion law. Therefore, the first motion equation can be written by using the forces acting on the vehicle in the x-axis direction in Equation (17) [22-24].

$$m\ddot{x} = (F_{fo} + F_{fi})\cos(\delta) + (F_{ro} + F_{ri}) - (D_{fo} + D_{fi})\sin(\delta) + my\ddot{\theta} \quad (17)$$

where *F* and *D* are the longitudinal and lateral forces of the front and rear outer and inner wheels. *m*, δ, and θ are the mass of the vehicle, the steering and sideslip angles of the EV, respectively.

The second motion equation is obtained according to the forces acting on the EV in the y-axis direction in Equation (18).

$$m\ddot{y} = (F_{fo} + F_{fi})\sin(\delta) + (D_{fo} + D_{fi})\cos(\delta) + (D_{ro} + D_{ri}) - mx\ddot{\theta} \quad (18)$$

The lateral sliding forces of the motion is calculated by [1].

$$D = -\alpha C \quad (19)$$

where *C* is the lateral stiffness coefficient. α is the slip angle which can be given for each wheel as follows.

$$\alpha_{fi} = \tan^{-1}\left(\frac{q_4 + q_6 l_f}{q_2 - \frac{d_r}{2} q_6}\right) - \delta \quad (20)$$

$$\alpha_{fo} = \tan^{-1}\left(\frac{q_4 + q_6 l_f}{q_2 + \frac{d_r}{2} q_6}\right) - \delta \quad (21)$$

$$\alpha_{ri} = \tan^{-1}\left(\frac{q_4 - q_6 l_r}{q_2 - \frac{d_r}{2} q_6}\right) \quad (22)$$

$$\alpha_{ro} = \tan^{-1}\left(\frac{q_4 - q_6 l_f}{q_2 + \frac{d_r}{2} q_6}\right) \quad (23)$$

The air friction resistance can be expressed by

$$F_S = 0.5\, d\, C_w\, AV^2 \quad (24)$$

where *d* and C_w are the density of the air and coefficient of the resistance. Besides, *A* and *V* are vertical cross-sectional area and the speed of the EV, respectively.

Control of the EV with four IW-PMSMs

Controlling each wheel of a four-wheel drive EV independently has a significant importance since the speed and torque of each wheel can be changed. Hence, a front-wheel drive or rear-wheel drive EV can be obtained if desired. However, these four wheels must work in harmony with each other to provide the balance of the EV. For this reason, the control of an EV with four in-wheel PMSMs is carried out as shown in Fig. 4. Here, the symbol * indicates the reference values.

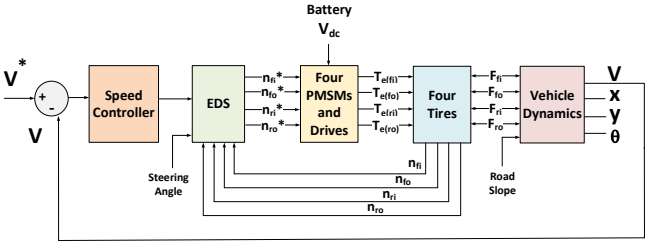

Figure 4. A dynamic model of an EV with PMSM with four in-wheel motors

In the system shown in Fig. 4, the difference between the speed taken from output of the vehicle dynamic model (*V*) and the reference speed the EV is passed through the speed control block using a PID controller. The speed obtained from the PID output is sent to the EDS. According to this EV speed value and steering angle, four wheel speeds are calculated by the designed EDS. When the steering angle is zero, it means the EV is traveling on a straight road. If it is different from zero, it turns right or left. Accordingly, the speed values of the right and left wheels will be different each other. In the proposed system, a PID controller is designed so that the difference in the wheel speed values taken from the EDS output is equal to the difference in the speeds taken from the real system. The designed system is illustrated for the front and rear wheels of the EV in Fig. 5. a and b, respectively.

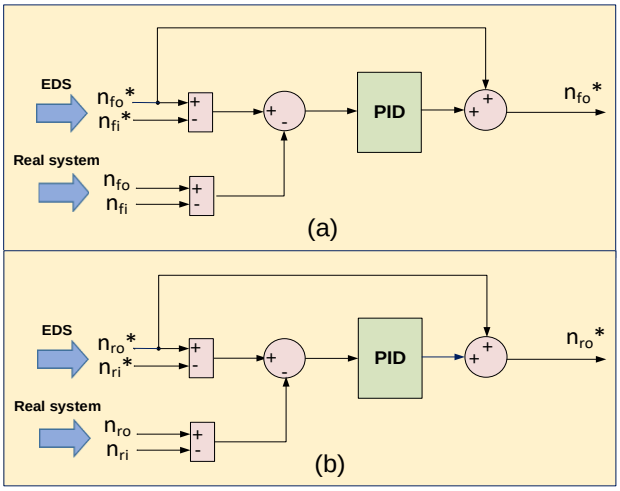

Figure 5. PID controller design using the speed differences for (a) the front wheels (b) rear wheels of the EV

As shown in Fig. 5, while the speed of one of the front or rear wheels is different from the desired speed value, the speed difference between the wheels will change. This disrupts the balance of the EV and prevents safe driving. Therefore, to ensure a stable driving of the EV on the road, a PID speed controller is designed to equalize the speed differences received from the real system and EDS. Then, the torque and forces of the four wheels are calculated by sending these optimal speed values to four PMSM drives.

In the proposed system, the load conditions of the PMSMs are examined based on the slope and curve of the road, the longitudinal and lateral forces of the EV are estimated. Lastly, the slope of the road, xy curve, and yaw angle θ are obtained from the longitudinal forces in the vehicle dynamics block. As a result, safe driving of the EV is provided by the designed system using a simple controller method based on various EV speeds and steering angles.

Results and Discussions

The dynamic model of a four-wheel drive EV is implemented in Matlab/Simulink. In this section, the results obtained from the designed model are presented. In the model, the reference speeds of the EV are taken as 50 km/h and 90 km/h. These speed values are compared with the speed value taken from the real system and passed through a PID controller. Accordingly, it can be seen in Fig. 6 that the actual speed value of the EV catches the reference speed.

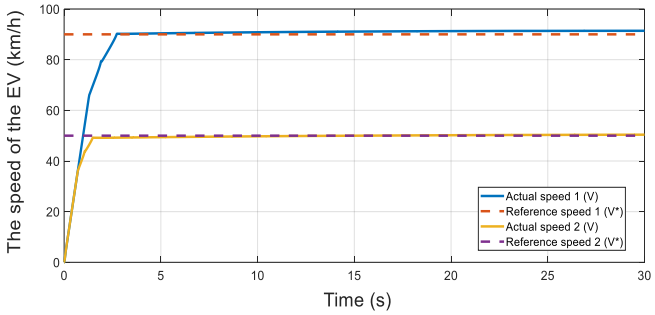

Figure 6. The actual speed curves of the EV for a) 50 km/h reference speed b) 90 km/h reference speed

In the model, the steering angle is taken as variable positive and negative values as shown in Fig. 7. Thus, the situations in which the vehicle travels on a straight road or the roads sloping to the right and left are examined.

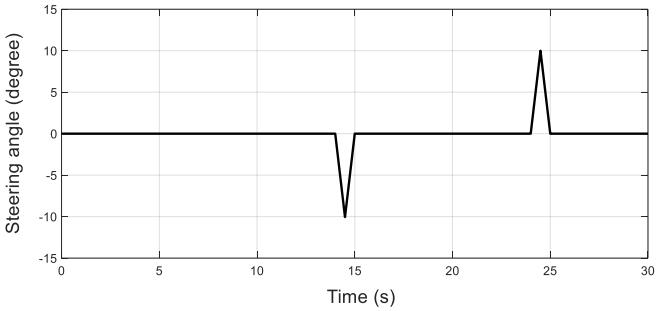

Figure 7. The change of the steering angle used in the dynamic model for 50 km/h reference speed of the EV

The road curve of the EV is drawn for the steering angle values and the reference speed value in Figure 8. As the steering angle changes, the path followed by the vehicle will also change. Accordingly, it is observed in Figure 8 that the EV moves safely on the given road profile.

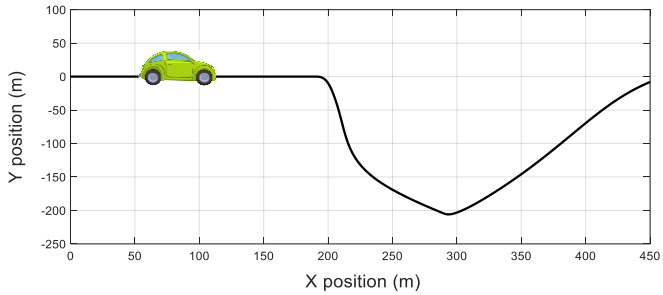

Figure 8. The road curve of the EV for different steering angles for 50 km/h reference speed of the EV

By using the designed EDS model, the four-wheel speeds of the EV are calculated depending on the steering angle and vehicle speed. The speeds calculated here are the reference speed values of the EV. Accordingly, the front inner and outer wheel speeds are shown in Fig. 9. In Fig. 9, n_f is the front wheel speed.

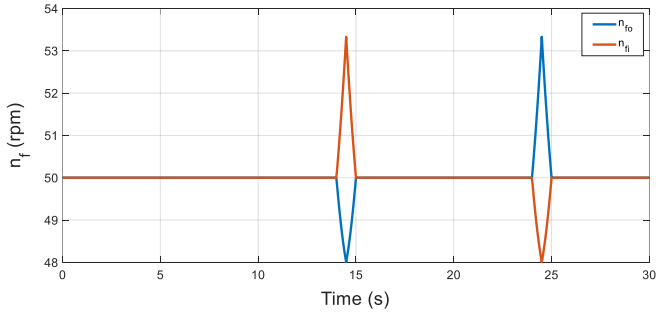

Figure 9. Front inner and outer wheel speeds calculated from the EDS for 50 km/h reference speed of the EV

Rear inner and outer wheel speeds are shown in Fig. 10. As illustrated in Fig. 10, n_r is the rear wheel speed.

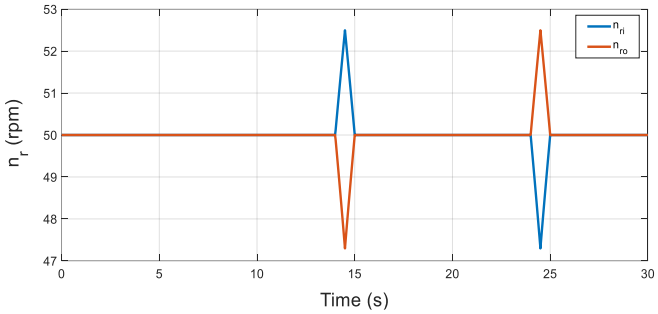

Figure 10. Rear inner and outer wheel speeds calculated from the EDS for 50 km/h reference speed of the EV

After the EDS is designed, the actual system of the EV consisting of vehicle dynamics is modeled. As the speed values taken from the real system change, the stability of the system will deteriorate. Hence, a PID controller is designed to compensate for this. A comparison for the front wheels of the EV is made between the reference speeds calculated by the EDS in the designed controller and the wheel speeds obtained by the real system without and with a controller as shown in Fig. 11.

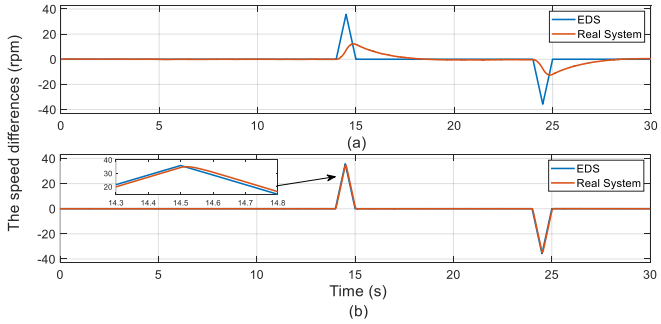

Figure 11. Speed differences of right and left front wheels of EDS and real system at 50 km/h reference EV speed for a) the system without controller b) the system with controller

As seen in Fig. 11, the difference between the front wheel speeds taken from the EDS output in the system without a controller is quite different from the speed differences taken from the output of the real system. On the other hand, in the system used a PID controller, this difference almost disappears and the stability of the EV is ensured.

Conclusion

In this study, a dynamic model of the EV with four IW-PMSMs is designed and the IW-PMSMs are controlled by the proposed PID controller. The simulation is realized by using MATLAB/Simulink. In the presented model, an EDS, four IW-PMSMs and their drives, tires and vehicle dynamic are placed. The load conditions of the motors are examined according to the slope of the road and all forces including longitudinal and lateral forces of the EV are estimated. Besides, an EDS is proposed for controlling the speed of the each wheel optimally based on the steering angle and the speed of the EV. After that, a PID controller is designed so that the speed differences of the real system are equal to the speed differences obtained from the EDS. Then, the change of each wheel speed are seperately examined and the road curve of the EV is drawn for various steering angles. The results show that the EV moves steadily on the road for different for bend slopes. Furthermore, the proposed controller is a simpler method than the other complex techniques in the literature such as fuzzy logic, artificial neural networks, and model predictive control, etc. As a result, all wheel speeds can be controlled optimally by this method.

Ethics committee approval and conflict of interest statement

There is no need to obtain permission from the ethics committee for the article prepared.

There is no conflict of interest with any person / institution in the article prepared.

References

[1] E. Esmailzadeh, G. R. Vossoughi, and A. Goodarzi, "Dynamic modeling and analysis of a four motorized wheels electric vehicle," *Vehicle System Dynamics*, vol. 35, no. 3, pp. 163-194, 2001.

[2] Z. Omac, M. Polat, E. Oksuztepe, M. Yildirim, O. Yakut, H. Eren, and H. Kurum, "Design, analysis, and control of in-wheel switched reluctance motor for electric vehicles," *Electrical Engineering*, vol. 100, pp. 865-876, 2018.

[3] T. Makhlouf, A. Achour, Y. Belkhier, and R. N. Shaw, "Design and control of an electric vehicle equipped with permanent magnet synchronous machine, " in *IEEE 4th International Conference on Computing, Power and Communication Technologies (GUCON)*, September 2021, pp. 1-5.

[4] P. Hang, F. Luo, S. Fang, and X. Chen, "Path tracking control of a four-wheel-independent-steering electric vehicle based on model predictive control," in *IEEE 36th Chinese Control Conference (CCC)*, July 2017, pp. 9360-9366.

[5] C. Zhao, W. Xiang, and P. Richardson, "Vehicle lateral control and yaw stability control through differential braking," in *IEEE International Symposium on Industrial Electronics*, vol. 1, July 2006, pp. 384-389.

[6] L. Xiong and Z. Yu, "Control allocation of vehicle dynamics control for a 4 in-wheel-motored EV," in *2nd International Conference on Power Electronics and Intelligent Transportation System (PEITS)*, vol. 2, December 2009, pp. 307-311.

[7] H. Zhou, H. Chen, B. Ren, and H. Zhao, "Yaw stability control for in-wheel-motored electric vehicle with a fuzzy PID method," in *IEEE The 27th Chinese Control and Decision Conference (CCDC)*, May 2015, pp. 1876-1881.

[8] C. Irimia, M. Grovu, G. M. Sirbu, A. Birtas, C. Husar, and M. Ponchant, "The modeling and simulation of an electric vehicle based on simcenter amesim platform," in *IEEE Electric Vehicles International Conference (EV)*, October 2019, pp. 1-6.

[9] K. Nam, S. Oh, H. Fujimoto, and Y. Hori, "Estimation of sideslip and roll angles of electric vehicles using lateral tire force sensors through RLS and Kalman filter approaches," *IEEE Transactions on Industrial Electronics*, vol. 60, no. 3, pp. 988-1000, 2012.

[10] S. Ding, L. Liu, and W. X. Zheng, "Sliding mode direct yaw-moment control design for in-wheel electric

vehicles," *IEEE Transactions on Industrial Electronics*, vol. 64, no. 8, pp. 6752-6762, 2017.

[11] Y. Tong, H. Jing, B. Kuang, G. Wang, F. Liu, and Z. Yang, "Trajectory tracking control for four-wheel independently driven electric vehicle based on model predictive control and sliding model control," in *IEEE 2021 5th CAA International Conference on Vehicular Control and Intelligence (CVCI)*, October 2021, pp. 1-5.

[12] C. Zhang, G. Yin, and N. Chen, "The acceleration slip regulation control for two-wheel independent driving electric vehicle based on dynamic torque distribution," in *IEEE 35th Chinese Control Conference (CC*C), July 2016, pp. 5925-5930.

[13] L. Zhai, T. Sun, and J. Wang, "Electronic stability control based on motor driving and braking torque distribution for a four in-wheel motor drive electric vehicle," *IEEE Transactions on Vehicular Technology*, vol. 65, no. 6, pp. 4726-4739, 2016.

[14] P. Pillay and R. Krishnan, "Modeling, simulation, and analysis of permanent-magnet motor drives. I. The permanent-magnet synchronous motor drive," *IEEE Transactions on Industry Applications*, vol. 25 no. 2, pp. 265-273, 1989.

[15] J. Yang, W. H. Chen, S. Li, L. Guo, and Y. Yan, "Disturbance/uncertainty estimation and attenuation techniques in PMSM drives—A survey," *IEEE Transactions on Industrial Electronics*, vol. 64, no. 4, pp. 3273-3285, 2016.

[16] O. Dal, M. Yildirim, and H. Kurum, "Optimization of permanent magnet synchronous motor design by using PSO," in *IEEE 4th International Conference on Power Electronics and their Applications (ICPEA)*, Sept. 2019, pp. 1-6.

[17] P. Pillay, R. Krishnan, "Modeling, simulation, and analysis of permanent-magnet motor drives, part I: The permanent-magnet synchronous motor drive," *IEEE Trans. Ind. Appl.*, vol. 25, pp. 265–273, 1989.

[18] G. Boztas, M. Yildirim, and O. Aydogmus, "Design and optimization of a PMSM for obtaining high-power density and high-speed," *Turkish Journal of Science and Technology*, vol. 15, no. 2, pp. 61-70, 2020.

[19] R. Krishnan, "Electric motor drives: modeling, analysis, and control," Prentice Hall, Inc., Upper Saddle River, New Jersey, 2001.

[20] S. Sriprang, B. Nahid-Mobarakeh, N. Takorabet, S. Pierfederici, N. Bizon, P. Kuman, and P. Thounthong, "Permanent magnet synchronous motor dynamic modeling with state observer-based parameter estimation for AC servomotor drive application," *Applied Science and Engineering Progress*, vol. 12, no. 4, pp. 286-297, 2019.

[21] M. Yildirim, E. Oksuztepe, and H. Kurum, "Design of electronic differential system for an electric vehicle with four independently controlled in-wheel PMSM," *Advances in Electrical & Computer Engineering*, vol. 24, no. 1, 2024.

[22] Y. Guodong, C. Zhe, and C. Jiansong, "Safety driving speed and lane keeping control for electric vehicle in variable curvature curve," in *IEEE 36th Chinese Control Conference (CCC)*, July 2017, pp. 9572-9577.

[23] K. Liu, J. Gong, A. Kurt, H. Chen, and U. Ozguner, "Dynamic modeling and control of high-speed automated vehicles for lane change maneuver," *IEEE Transactions on Intelligent Vehicles*, vol. 3, no. 3, pp. 329-339, 2018.

[24] J. E. Esquivel-Cruz, F. Beltran-Carbajal, I. Rivas-Cambero, Z. Damián-Noriega, G. Alvarez-Miranda, and R. Pérez-Moreno, "Tracking control approach of speed profiles of induction motors used in electric vehicle," in *IEEE 11th International Conference on Smart Energy Grid Engineering (SEGE)*, August 2023, pp. 22-26.